J. Membrane Biol. 140, 13–30 (1994)

The Journal of
Membrane
Biology

Elevation in Intracellular Calcium Activates Both Chloride and Proton Currents in Human Macrophages

K.O. Holevinsky, F. Jow, D.J. Nelson

Departments of Medicine and Neurology and the Committee on Cell Physiology, The University of Chicago, Chicago, Illinois 60637

Received: 10 August 1993 / Revised: 31 January 1994

Abstract. The transition of a resting macrophage into the activated state is accompanied by changes in membrane potential, cytoplasmic pH, and intracellular calcium (Ca_i). Activation of Cl^- as well as H^+-selective currents may give rise to stimulus-induced changes in membrane potential and counteract changes in intracellular pH (pH_i) which have been observed to be closely associated with respiratory burst activation and superoxide production in macrophages. We carried out whole-cell voltage clamp experiments on human monocyte-derived macrophages (HMDMs) and characterized currents activated following an elevation in Ca_i using isosmotic pipette and bath solutions in which Cl^- was the major permeant species. Ca_i was elevated by exposing cells to the Ca^{2+} ionophore A23187 (1–10 μM) in the presence of extracellular Ca^{2+} or by internally exchanging the patch-electrode solution with ones buffered to free Ca^{2+} concentrations between 40 and 2,000 nM. We have identified two Ca^{2+}-dependent ion conductances based on differences in their characteristic time-dependent kinetics: a rapidly activating Cl^- conductance that showed variable inactivation at depolarized potentials and a H^+ conductance with delayed activation kinetics. Both conductances were inhibited by the disulfonic acid stilbene DIDS (100 μM). Current activation for both Ca^{2+}-dependent conductances was phosphorylation dependent, neither conductance appeared in the presence of the broad spectrum kinase inhibitor H-7 (75 μM). Inclusion of the autophosphorylated, Ca^{2+}/calmodulin-dependent protein kinase in the pipette in the presence of ATP induced a rapidly activating current similar to that observed following an elevation in Ca_i. Activation of both conductances would contribute to the changes in membrane potential which accompany stimulation-induced activation of macrophages as well as counteract the decrease in pH_i during sustained superoxide production.

Key words: Chloride channels — Human macrophage — Ca^{2+}-calmodulin-dependent protein kinase II — Macrophage activation — Hydrogen ion current — pH regulation

Introduction

Activation of phagocytic cells occurs following the binding of soluble and particulate ligands to cell membrane receptors. Early events that occur following ligand binding include changes in membrane potential, ion fluxes, and alterations in levels of cytosolic calcium (Ca_i) and cytosolic pH (pH_i). Transient increases in Ca_i that occur during adherence (Kruskal & Maxfield, 1987), phagocytosis (Lew et al., 1985; Jaconi et al., 1990) and the binding of soluble ligands e.g., platelet activating factor to macrophage surface receptors (Conrad & Rink, 1986) have been shown to activate K^+ channels (Gallin, 1984, 1989; Nelson, Jow & Jow, 1990; Hara et al., 1991; Randriamampita, Bismuth & Trautmann, 1991) as well as nonselective cation channels (Lipton, 1986; Katnik & Nelson, 1993) in macrophage membranes. Large conductance chloride (Cl^-) channels, absent in resting macrophages, can be elicited by exposure of peritoneal macrophages to the phagocytic stimulus zymosan during cell-attached recordings (Kolb & Ubl, 1987). In the studies of Kolb and Ubl (1987), large conductance anion channel activation could also be mimicked by the addition of A23187 to Ca^{2+}-containing solutions, thus suggesting the presence of a third

Correspondence to: D.J. Nelson, The University of Chicago, Department of Neurology, MC2030, 5841 S. Maryland Ave., Chicago, Illinois 60637

class of channels controlled via changing levels of internal Ca_i.

We examined Ca^{2+}-stimulated whole-cell currents in the in vitro differentiated macrophage . We observed currents which were of two kinetic types: a rapidly activating current which was sensitive to changes in external Cl^- concentration and a second current with delayed activation kinetics which was insensitive to changes in external Cl^-.

Activation of the rapidly activating Ca^{2+}-dependent Cl^- current in macrophages is via phosphorylation by the multifunctional Ca^{2+}/calmodulin-dependent protein kinase (CaMKII). We demonstrate that intracellular application of the isolated, activated kinase elicits a Cl^- current similar in its kinetic phenotype to that seen in the presence of the calcium ionophore A23187.

The selectivity of the Ca^{2+}-dependent, slowly activating current indicated that H^+ was the charge carrier. Proton conductances have been described in a variety of cell types including neurons (Byerly, Meech & Moody, 1984), oocytes (Barish & Baud, 1984), alveolar cells (DeCoursey, 1991), and neutrophils (DeCoursey & Cherny, 1993). Activated phagocytic cells undergoing a respiratory burst produce intracellular acid and must secrete protons to regulate internal pH. The slowly activating outward current observed following an increase in Ca_i in our studies is the first report of a proton conductance capable of mediating proton efflux in human monocyte-derived macrophages (HMDMs).

The present work examines the Ca^{2+}-dependent activation of both Cl^- and H^+ currents in HMDMs. Evidence is presented demonstrating that both conductances are sensitive to the disulfonic acid stilbene DIDS and that the activation of both conductances is phosphorylation dependent. Proton conductance activation in HMDMs may be indirect and involve stimulation of Ca^{2+}- and phosphorylation-dependent metabolic acid production.

Materials and Methods

Mononuclear cells from normal human blood were separated from neutrophils and erythrocytes by Ficoll-Hypaque density gradient centrifugation as previously described (Nelson, Jow & Jow, 1990). Cells isolated from the mononuclear fraction were washed three times with RPMI-1640 growth medium, resuspended in RPMI-1640 supplemented with 10% autologous human serum, and plated at a density of 1×10^6 cells/ml on uncoated 35 mm tissue culture dishes which had been finely scored with a fine wire brush. The scoring of the tissue culture dishes greatly aided growth and long-term differentiation in culture. After one hour incubation, the adherent cells were washed three times with non-serum-containing RPMI-1640. Adherent cells were incubated with serum-containing medium, which was replaced the day following the isolation procedure.

Alternatively, human monocyte-enriched leukocyte fractions, suspended in RPMI-1640 containing 10% autologous human serum, 100 U/ml penicillin and 50 μg/ml streptomycin were cultured in Teflon vials (Savillex, Minnetonka, MN) at 37°C in a 5% CO_2 air atmosphere prior to their introduction into adherent culture.

Electrophysiology

Whole-cell recordings from HMDM membranes were obtained using the techniques of Hamill et al. (1981). A dish containing cultured cells was placed in a chamber on the movable stage of an inverted microscope equipped with phase-contrast optics. Recording pipettes were formed from soda lime glass (Blue-Dot Hematocrit Glass; Fisher Scientific, Pittsburgh, PA) using a horizontal puller (Model P-87, Sutter Instruments, San Rafael, CA). Experiments were performed at room temperature (21–23°C).

Whole-cell currents were obtained using a List EPC-7 (List Electronic, Darmstadt, Germany) voltage clamp. In general, voltage pulses of 1.7 sec in duration were delivered once every 10 sec. The interpulse interval was sufficient to allow for recovery from the effect of the preceding pulse. The output of the current-to-voltage converter was filtered through a low pass filter at 500 Hz. The current signal was sampled at 1 kHz by a 12 bit A/D converter (Data Translation 2818, Marlborough, MA) and written into data files using an IBM-AT. Summary data are expressed as means ± standard error of the mean with the number of experiments in parentheses.

Solutions

The bath solution contained (in mM): 140 *N*-methyl-D-glucamine (NMDG)-Cl, 2 $CaCl_2$, 2 $MgCl_2$, and 10 *N*-2-hydroxy-ethylpiperazine-*N'*-2-ethanesulfonic acid (HEPES) buffered to pH 7.4. The pipette solution contained: 40 NMDG-Cl, 100 NMDG-glutamate, 2 $MgCl_2$, 1 Mg-ATP, 10 HEPES and a Ca-EGTA buffer to yield a desired free Ca^{2+} concentration buffered to pH 7.2. The $CaCl_2$ and EGTA composition of the internal solutions varied according to experimental protocol. Ca-EGTA buffer solutions were prepared according to the procedure described by Neher (1988): A solution of 200 mM EGTA was neutralized with a NMDG-OH to a pH of 6.5. A portion of this solution was diluted twofold, neutralized with NMDG-OH to a final pH of 7.2, and stored as 100 mM Ca^{2+}-free EGTA stock solution. A second stock solution was prepared by adding 200 mM $CaCl_2$ to the 200 mM Ca^{2+}-free EGTA stock solution and titrating with NMDG-OH back to pH 7.2. The Ca^{2+}-EGTA buffer solution was diluted to a final concentration of 100 mM and titrated back to pH 7.2. Both solutions were stored at 4°C. Ca-EGTA buffered pipette solutions were made by adding aliquots of the two stock solutions of 100 mM Ca^{2+}-EGTA and 100 mM NMDG-EGTA to the Ca-EGTA free pipette solution to achieve the desired final free Ca^{2+} concentration. Using this procedure, we did not observe large shifts in pH which normally occur when $CaCl_2$ is added directly to EGTA-containing solutions. The free Ca^{2+} concentration was calculated assuming an apparent dissociation constant of the Ca-EGTA complex of 0.15 μM at pH 7.2 using the methodology of Fabiato and Fabiato (1979). Composition of the pipette solutions with varying Ca^{2+}-buffering capacities are given in Table 1. Solution osmolarities were monitored using a vapor pressure osmometer (Model 5500, Wescor, Logan, UT).

Superfusion of the cells was performed by exchanging the bath at a rate of 3cc/min via a gravity feed superfusion system. In specific experiments, intrapipette solutions were exchanged during the recording period using the method of Soejima and Noma (1984).

The selectivity of the currents was determined by replacing the NMDG-Cl in the bath solution with an isosmolar amount of an appropriate NMDG salt. In those experiments where the halide composition of the solution was changed, the ground electrode was con-

Table 1. Calcium buffer composition of internal pipette solutions of varying buffering capacity

Calculated free-Ca^{2+} (nM)	Buffering Capacity	Free EGTA (mM)	Ca^{2+}-EGTA (mM)
34	Low	0.3	0.05
100	Low	0.45	0.16
345	Low	0.45	0.30
43	High	1.0	0.20
39	High	11.0	2.0
100	High	11.0	4.0
200	High	11.0	6.0
500	High	11.0	8.0
1,080	High	11.0	9.5
2,000	High	11.0	10.2

Free Ca^{2+} was calculated assuming an apparent dissociation constant for EGTA of 0.15 μM at pH 7.2 using the methodology of Fabiato and Fabiato (1979).

nected to the bath solution via an agar salt bridge to minimize electrode junction potentials.

DIDS (4′,4′-diisothiocyanatostibene-2′,2′-disulfonic acid), the Ca^{2+} ionophore A23187, H-7 (1-(5-isoquinolinylsulfonyl)-2 methylpiperazine (dihydrochloride)), Mg-ATP, and ATP-γ-S were purchased from Sigma (St. Louis, MO). The Ca^{2+} ionophore, A23187, was solubilized in DMSO and stored as a 10 mM stock solution at −20°C. Aliquots of the 10 mM stock A23187/DMSO solution were diluted to a final concentration of 1–10 μM in NMDG-Cl bath solution just prior to use (final DMSO concentration less than 0.1%). Voltage clamped cells were acutely exposed to the ionophore via bath solution exchange during the electrophysiological recordings.

The multifunctional Ca^{2+}-calmodulin dependent protein kinase (CaMKII) purified from rat brain, a generous gift from H. Schulman (Stanford University, Stanford, CA), was aliquoted, stored at −80°C in 25 mM Tris-HCl (pH 7.4), 1 mM EGTA, 100 mM NaCl, and 10% glycerol. The kinase was prepared for the electrophysiological experiments according to previously published methodology (Nishimoto et al., 1991; Wagner et al., 1991) and delivered to the cell interior via inclusion in the patch pipette solution. The purified kinase was thawed and made autonomous by the incubation of 100 μg/ml CaMKII with 600 μM calmodulin, 500 μM ATP-γ-S, and 1 mM $CaCl_2$ for 10 min at 4°C immediately before the patch clamp experiments were performed. The reaction was terminated by addition of 20 mM EDTA. The mixture was diluted fivefold with the pipette buffer solution and kept on ice. In experiments in which cells were dialyzed with the activated kinase, the tip of the pipette was prefilled with kinase-free pipette solution after which approximately 10 μl of activated kinase solution (approximately 20 μg/ml) was sandwiched between kinase-free pipette solution. Failure to prefill the tip of the pipette with kinase-free solution resulted in a significant reduction in the rate of seal formation.

All experiments were carried out at room temperature. Where a multiple number of experiments were performed for a given experimental condition, data are expressed as means ± SEM with the number of experiments in parentheses.

Cell Loading with Fluorescent Probes

Cells were maintained in suspension culture and plated on glass-bottom culture dishes approximately 4–8 hr prior to recording. Dishes, which served as recording chambers, were constructed as follows: an 18 mm diameter hole was punched into the bottom of a 35 mm plastic culture dish. A 22 × 22 mm, acid-cleaned coverslip was fixed to the outside surface of the dish covering the hole, using Sylgard 184 silicone elastomer (Dow-Corning, Midland, MI). Dishes were placed in a drying oven at 55°C for 1 hr to allow for sufficient Sylgard curing and sterilized with 70% ethanol immediately prior to use. A drop of the mononuclear cell suspension (0.1 ml) was placed in the center of the exposed coverslip and incubated for 1 hr at 37°C in a humidified 5% CO_2:95% O_2 environment. Following incubation and initial cell attachment, cells were washed twice with HBSS buffered with 10 mM HEPES. Cells were loaded with BCECF (5 μM) in HBSS buffered with 10 mM HEPES for 20 min at room temperature. This loading solution also contained 0.1% bovine serum albumin (BSA) to prevent nonspecific dye binding. Following the loading procedure, cells were washed and incubated for 30 min in HBSS with 10 mM HEPES, pH 7.4 to allow time for maximal dye desterification. Cells were washed again prior to use. All experiments were performed within 2 hr after completion of BCECF loading.

Microfluorimetry

Dye excitation illumination was provided by a Photon Technology International (PTI) D-104 dual wavelength illumination system. The D-104 consisted of a 75 W Xenon arc lamp, a variable speed reflective optical chopper under computer control which alternated the excitation illumination between 440 and 495 nm through two optical filters. The illumination system was coupled to the microscope via a fiber optic cable. Excitation light was deflected with a 510 nm dichroic mirror through a 40× phase (Nikon Fluor, N.A. 0.85) fluorescence objective. Emitted fluorescence filtered at 520 nm was collected by a Hammamatsu R928 photomultiplier tube and photon-counting photometer through a variable rectangular aperture roughly equal to the area of the single cell. Photomultiplier output was sampled at 10 Hz and processed using a PTI interface on a NEC 386/20 personal computer.

Results

Ca^{2+}-dependent Current Activation

HMDMs which had been maintained in culture for up to three weeks were studied under whole-cell voltage clamp. Experiments were performed using pipette and bath solutions containing NMDG as a Na^+ and K^+ replacement, and Cl^- as the major permeant ion. Experiments were performed in asymmetrical Cl^- solutions (Nernst potential for Cl^- in these studies was −30 mV). We studied Ca^{2+}-dependent conductance activation in macrophages in response to an elevation in Ca_i, elicited either by exposure of the cells to the Ca^{2+} ionophore A23187 or by dialysis of the cell with pipette solutions buffered to free Ca^{2+} concentrations of between 40 and 2,000 nM. We omitted K^+ from our experimental solutions since Ca^{2+}-activated K^+ conductances in macrophages have been extensively characterized elsewhere (Gallin, 1984; 1989; Randriamampita & Trautmann, 1987; Gallin & McKinney, 1988; Nelson et al., 1990). In the presence of extracellular Ca^{2+}, A23187 (1–10 μM) induced significant current activation. When iono-

phore was introduced in a nominally Ca^{2+}-free solution, no significant current increase was observed ($n = 2$, *data not shown*), indicating that elevated intracellular Ca^{2+} via the Ca^{2+} ionophore was responsible for the current activation.

Current activation in the absence of a Ca^{2+} stimulus was not observed. In the unstimulated cell with pipette solutions containing less than 45 nM free Ca^{2+} using both high and low buffering capacity pipette solutions (*see* Table 1), the average current at the most depolarized potential of 100 mV showed a slight decrease over time. The mean change in current amplitude over a control recording period of up to 45 min was -68 ± 65 pA ($n = 25$).

An increase in Ca_i resulted in an increase in current amplitude across the voltage range (Fig. 1). The time course required to achieve maximal levels of current activation was variable and occurred over 10 to 20 min following membrane disruption with pipette solutions buffered to free Ca^{2+} levels above 100 nM, as well as after exposure of the cells to A23187. The pipette free Ca^{2+} concentration required to elicit voltage-dependent current activation was also variable. Two classes of ion-selective currents were observed regardless of the method used to increase Ca_i. The two Ca^{2+}-dependent ion conductances could be distinguished on the basis of the time dependence of current activation. Representative Ca^{2+}-dependent currents activated in the presence of 10 μM A23187 are shown in Fig. 1. The peak current-voltage (*I-V*) relationship for the currents showing rapid activation (Fig. 1*A–C*) showed moderate rectification as would be expected in asymmetrical Cl^--containing solutions. The peak current-voltage (*I-V*) for the second current type (Fig. 1*D–F*), a slowly activating conductance, was characterized by prominent outward rectification. The presence of voltage-dependent inactivation associated with the rapidly activating currents was highly variable and currents often appeared time independent.

In general, currents activated in the presence of high Ca^{2+} buffering capacity pipette solutions (1–11 mM EGTA) showed rapidly activating kinetics (Fig. 1*A–C*). The rapidly activating conductance was observed in 85% ($n = 88$) of the cells where current activation was brought about with pipette solutions of high Ca^{2+} buffering capacity. The mean increase in whole-cell current for cells expressing the rapidly activating currents was 946 ± 99 pA ($n = 51$). In contrast, currents elicited from cells dialyzed with the solutions of low Ca^{2+} buffering capacity (0.3–0.45 mM EGTA) generally showed delayed activation kinetics in the depolarizing range (as in Fig. 1*D–F*). The mean increase in whole-cell current at 100 mV for the delayed conductance following activation was 624 ± 98 pA ($n = 25$). Currents with a delayed time course were observed in 82% ($n = 38$) of the cells following an elevation in Ca_i in the presence of low Ca^{2+} buffering capacity pipette solutions. The remaining cells activated under either Ca^{2+} buffering conditions exhibited the alternative current type. Although there was an apparent trend in the dependency of the current kinetic type on the Ca^{2+}-buffering capacity of the solution, the dependency was not absolute and, therefore, further separation of the currents based on the buffering capacity of the internal solutions was not made.

Current Activation is Dependent upon Culture Conditions

The fraction of cells which expressed a Ca^{2+}-dependent conductance showed an apparent dependence upon cell adherence as well as soluble factors in the culture media. Only 76% ($n = 168$) of the cells which had been maintained in adherent culture following isolation exhibited either type of Ca^{2+}-dependent current. The percentage of cells responding to an increase in Ca_i with current activation increased to 91% ($n = 23$) if cells were maintained in suspension culture and plated 1 hr prior to the electrophysiological experiments. In unresponsive, long-term adherent cultures, the percentage of responsive cells increased to 71% ($n = 17$ from six separate isolations) if the culture medium was changed approximately 24 hr prior to the electrophysiological experiments.

Selectivity

The ion selectivity of the two classes of Ca^{2+}-dependent currents was determined in experiments in which Cl^- in the bathing solution was replaced with a series of halide anions and aspartate. In cells exposed to pipette and bath solutions containing 40 and 140 mM Cl^-, respectively, the current reversal potential following an elevation in Ca_i was -15.1 ± 1.6 mV ($n = 47$) for the rapidly activating current and -12.8 ± 4.2 mV ($n = 25$) for the current with delayed activation kinetics. When aspartate was substituted for all but 8 mM of the external Cl^-, the current reversal potential shifted in the depolarizing direction by 11.8 ± 8 mV ($n = 3$) for the slowly activating current and 35.2 ± 2.3 mV ($n = 3$) for the rapidly activating current. Results from representative experiments for each current type are given in Fig. 2*A* and *B*. Reversal potential measurements indicated that aspartate is 0.25 times as permeant as Cl^- for the rapidly activating current and 0.7 times as permeant as Cl^- for the slowly activating current as calculated from the Goldman-Hodgkin-Katz equation. A large outward current remained in the presence of aspartate for the delayed conductance which was not seen for the rapidly activating Cl^- conductance (g_{Cl}) indicating that Cl^- was unlikely to be the current carrier for the delayed out-

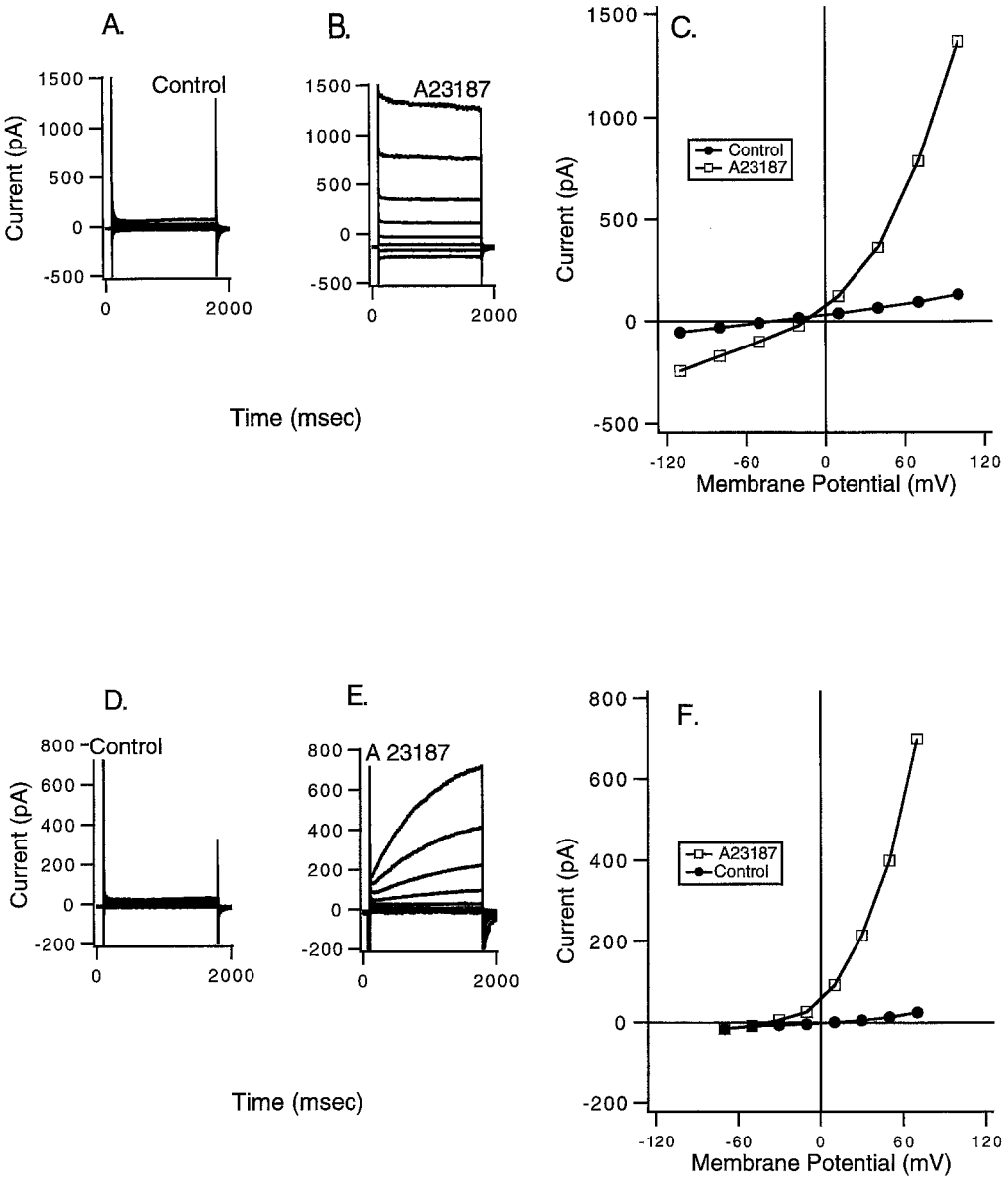

Fig. 1. Two kinetically distinct families of currents activated following exposure of HMDMs to 10 μM A23187 in solutions in which all Na^+ and K^+ had been isosmotically replaced with NMDG. (*A–C*) Rapidly activating current induced in the presence of a high Ca^{2+} buffering capacity intracellular solution containing 1 mM EGTA and 0.2 mM Ca^{2+}. Hyperpolarizing and depolarizing pulses 1.7 sec in duration were applied at 10 sec intervals from a holding potential of −60 mV to potentials between −110 and +100 mV in 30 mV intervals. (*A*) Whole-cell currents prior to activation. (*B*) Currents induced by 10 min exposure to A23187 (10 μM). (*C*) Peak *I-V* relationship for baseline currents under control conditions (filled circles) and after exposure of the cell to 10 mM A23187 (open squares). Current amplitude was determined within 32 msec following the initiation of the voltage pulse. (*D–F*) Delayed outward current activated in the presence of a low Ca^{2+} buffering capacity intracellular solution containing 0.45 mM EGTA and 0.3 mM Ca^{2+}. In this record, the command voltage was stepped from −70 mM to +70 mV in 20 mV increments. (*D*) Control current recording. (*E*) Currents activated after 20 min exposure to A23187 (10 μM). (*F*) Peak *I-V* relationship for the current under control conditions (filled circles) and following activation with 10 mM A23187 (open squares). Current amplitude was determined at 1,680 msec. The zero current potential for the cell in *A–C* was −38.8 mV under prior exposure to the ionophore and −15.4 mV following maximal current activation. The zero current potential for the cell in *D–F* was −37.9 mV before and −27.8 mV after maximal A23187-induced current activation. The predicted E_{Cl} in these experiments was −31 mV.

ward conductance. The selectivity among halide anions for the two classes of Ca^{2+}-dependent conductances was determined in experiments in which bath NMDG-Cl was replaced by equimolar amounts of NMDG-I or NMDG-Br. The relative halide permeability for the rapidly activating conductance was $I^- > Br^- = Cl^- \gg$ aspartate, as given in Table 2. The relative halide permeability for the delayed activating current showed no

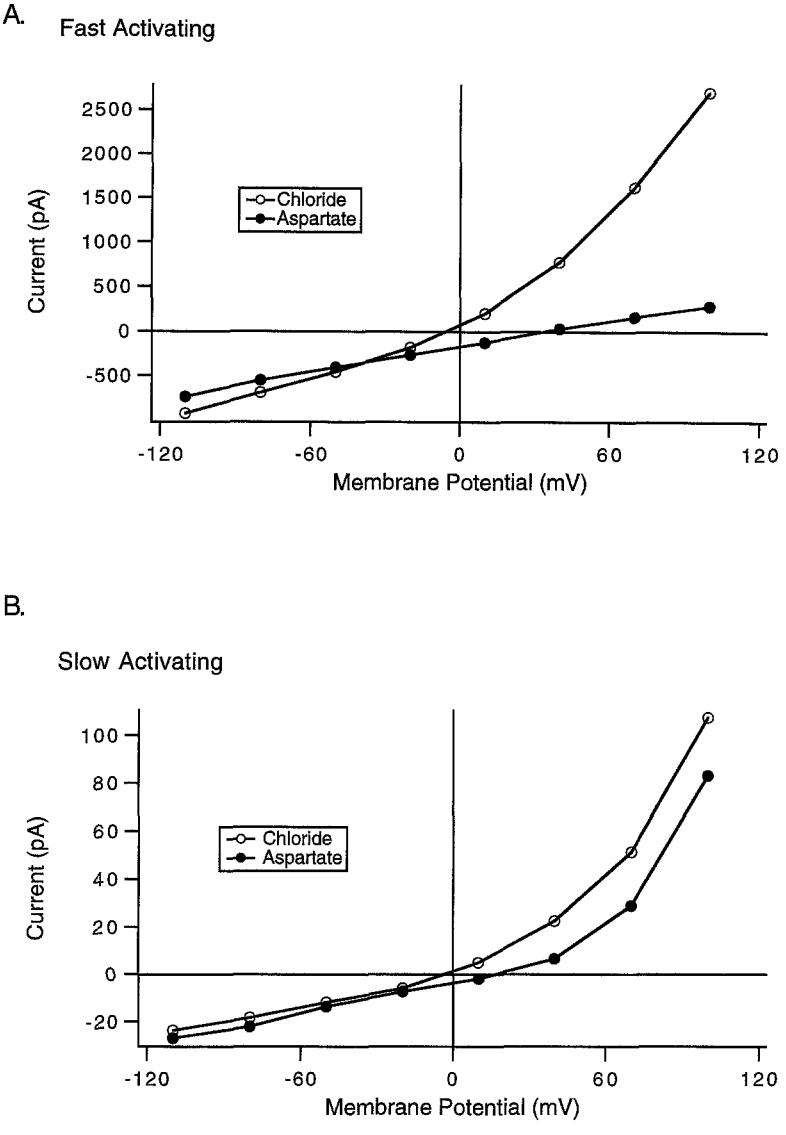

Fig. 2. Effect of replacing most of the external Cl^- by aspartate. (*A*) *I-V* relationship for the rapidly activating Cl^- current before (open circles) and after (filled circles) exchange of the external solution for one in which all but 8 mM of the external solution Cl^- had been replaced with aspartate. The current reversal potential following the aspartate substitution was +33.9 mV indicating that the current was predominantly Cl^- selective. (*B*) *I-V* relationship for the slowly activating current after a similar exchange of aspartate for Cl^- in the external solution; open circles correspond to currents in the presence of Cl^-, filled circles correspond to currents measured in the presence of the aspartate solution. The reversal potential in the aspartate solution was +17.4 mV. The large outward conductance following the aspartate solution exchange indicated that an ion other than Cl^- was the permeant species carrying the delayed outward current. A reversal potential of +60 mV following the aspartate substitution would have been predicted for a perfectly Cl^- selective current. Ca^{2+}-dependent currents in both cells were activated in the presence of 5 μM A23187.

significant differences in permeability of the channel to I^-, Br^-, or aspartate, with respect to Cl^-.

H^+ Selectivity of the Delayed Outward Current

The negligible anion selectivity of the slowly activating current suggested that it might be carried by an ion other than Cl^-. We speculated that the current might be carried by protons, given the similarity in kinetic profile to the proton currents described in neutrophils (DeCoursey & Cherny, 1993) and the ionic composition of the bath and pipette solutions. To test this hypothesis, we examined whether we could mimic current activation in solutions in which the driving force for protons was enhanced.

Figure 3 illustrates Ca^{2+}-dependent current activation in an experiment in which the internal/pipette pH_i was 5.51. Current activation following exposure of the cell to 5 μM A23187 appeared to be similar to that in which pipette and bath solutions were buffered to neutral pH (Fig. 1*A*). Replacement of the bath solution with one in which all but 6 mM Cl^- was replaced with 140 Na-glutamate at pH 7.4 revealed an underlying current with time-dependent activation kinetics. The reversal potential (E_{rev}) of the delayed current obtained from families of tail currents was −38 mV, as seen in the instantaneous current voltage-relationship in Fig. 3*D*. The predicted reversal potential in these solutions for a H^+-selective current was −48 mV indicating that the slowly activating current is carried predominantly by H^+. The E_{rev} was significantly more positive than E_H as has been observed for H^+ currents in rat alveolar cells (DeCoursey, 1991), and in this experiment could be accounted for if the cytoplasmic pH was 5.9 instead of 5.5.

Table 2. Comparative halide permeability of both Ca^{2+}-activated conductances

Conductance type	P_I/P_{Cl}	P_{Br}/P_{Cl}	P_{asp}/P_{Cl}
Rapidly activating	1.47 ± 0.12 (11)	1.03 ± 0.04 (11)	0.25 ± 0.02 (3)
Slowly activating	1.30 ± 0.42 (3)	1.08 ± 0.14 (3)	0.70 ± 0.24 (3)

Values are expressed as means ± SEM. Halide selectivity experiments were performed by replacement of the bath solution containing 100 mM NMDG-Cl with an appropriate NMDG salt. Sucrose was added to the bath solution to correct for differences in osmolarity. The relative permeabilities were determined using the relationship $P_X/P_{Cl} = [Cl]_i/[X]_o \exp -(E_R F/RT)$, where P_X/P_{Cl} is the permeability ratio of the test anion X relative to Cl^- and E_R is the current reversal potential. The relative halide permeability was determined for all three halides in each of 11 cells for the rapidly activating current and in 3 cells for the slowly activating current. The aspartate substitution experiments, in which all but 8 mM Cl^- in the external solution was replaced, were done using separate cells in which 140 mM NMDG-Cl was replaced with NMDG-aspartate.

Therefore, further experiments were carried out on cells loaded with the pH-sensitive dye BCECF to monitor internal pH as a direct consequence of prolonged increases in Ca_i and in response to dialysis of the cell with a pipette solution of known pH.

Cells were loaded with BCECF and pH changes were measured following whole-cell formation and as a consequence of exposure to the ionophore. The pipette solution in these experiments was pH 7.2 and contained 342 nM free Ca^{2+}. A total of 12 cells were examined for pH changes following whole-cell formation. In three cells, we observed an acidification in the internal pH from 8.0 to 5.6 following whole-cell formation. Further stimulation with the ionophore in the same three cells failed to significantly alter pH_i beyond that observed as a consequence of whole-cell formation. In two cells, the pH shift was in the alkalinizing direction from 7.1 to 7.4. In the remaining seven cells which were examined, we observed a transient alkalinization followed by a slow acidification. At the time of the alkalinizing shift, we sometimes observed the activation of a current which was similar in its kinetics to the slowly activating current. Slowly activating currents were not observed in other cells exhibiting an alkalinizing shift, possibly due to the transient nature of the current or because the currents were underlying a Cl^- current.

Although the slowly activating current could be observed in cells with high Ca_i and neutral pH, it was more frequently seen in cells which were studied in the presence of an acidic pipette solution with a pH of 6.0 or below. Tail current experiments were performed on BCECF-loaded cells exhibiting the slowly activating current in the presence of known proton gradients to determine if the current was indeed carried by protons. In the experiment depicted in Fig. 4*A*, the internal pH was 6.0 and the external pH was 7.4, which would predict a current reversal potential of −35 mV. The pH_i, as indicated by the BCECF fluorescence ratio, was 7.0 at the point at which the tail currents were observed. The BCECF data predicts an E_H of −10 mV, equivalent to the experimentally observed E_{rev} of −12.5 mV obtained from the family of tail currents. In the experiment illustrated in Fig. 4*B*, the pipette pH was 7.2 and the external pH was 7.4. The pH_i as monitored directly was 7.8 at the time the tail currents were obtained. The predicted E_H was 10.1 mV and the experimentally observed E_{rev} was 10 mV. The E_{rev}, as obtained from the tail current data when compared to the predicted E_H using the observed pH_i, indicates that H^+ is the main charge carrier for the slowly activating current. It should be noted that it is equally probable that hydroxyl ions may be the current carrier and that our data do not differentiate between these two possibilities. However, lacking evidence to the contrary, the conductance will be henceforth referred to as H^+ selective.

It should be noted that if the pH of the pipette solution had been used as pH_i in the calculation of the theoretical E_H instead of the pH_i as determined directly from the fluorescence data, the predicted E_H for the solutions in the experiments described in Fig. 4 would have been −35.4 and −5.0 mV for the acidic and neutral solutions, respectively. The deviation in the experimentally determined values for E_{rev} from that predicted using the pH of the pipette solution in the calculation of E_H reflects the ability of the cell to regulate its pH_i in the presence of cytoplasmic dialysis via a pH-buffered pipette solution.

The maximum H^+ current obtained at +110 mV and a pH_i of 6.0 when normalized to cell capacitance yielded a current density of 1.13 ± 0.22 pA/pF (n = 3). This value is lower than the current densities reported for human neutrophils (17.1 pA/pF; DeCoursey & Cherny, 1993), the alveolar epithelial cell using high internal pH buffer concentrations (27.3 pA/pF; DeCoursey, 1991) and snail neurons (14.6 pA/pF: Byerly & Suen, 1989).

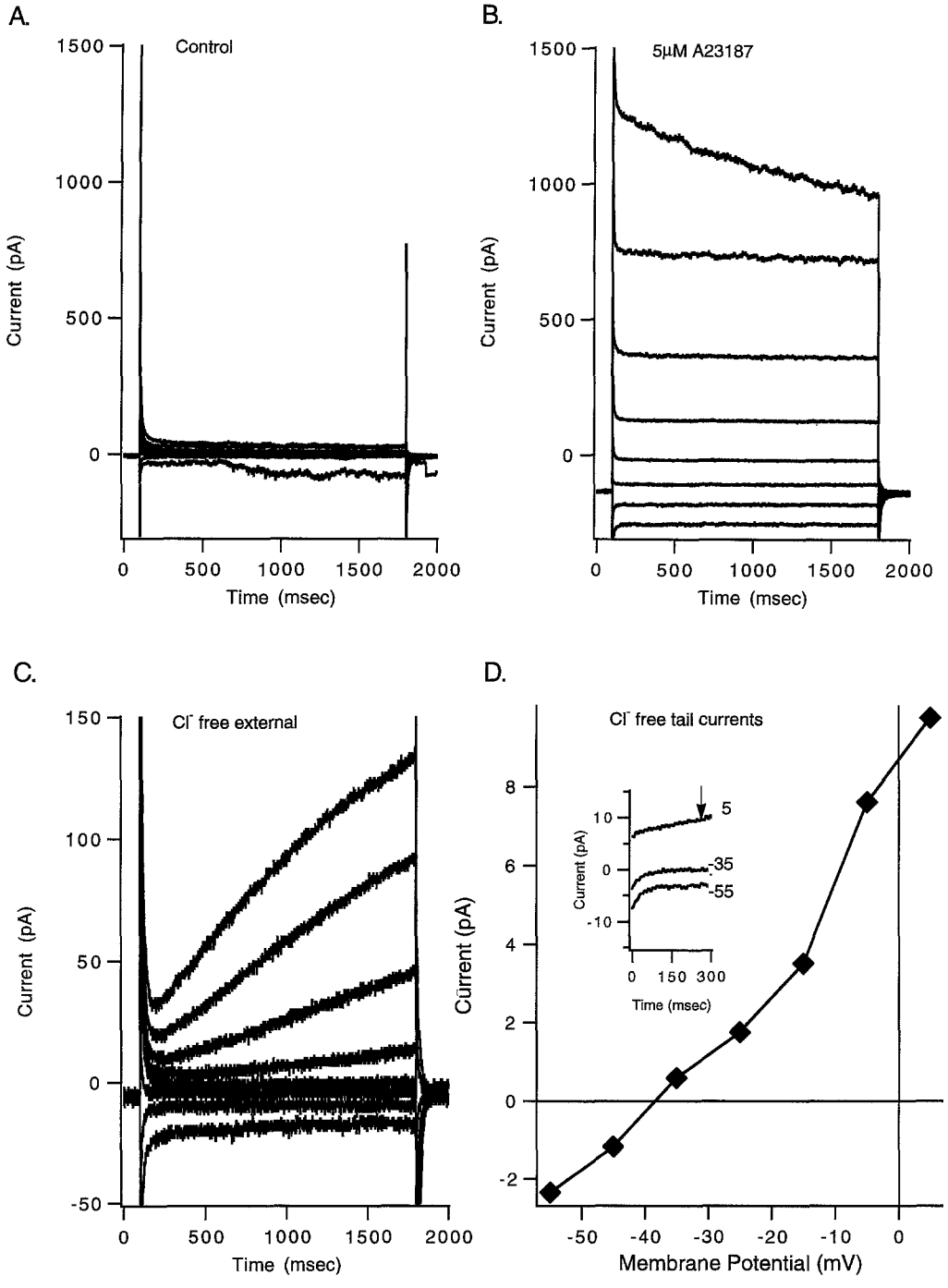

Fig. 3. Ca^{2+}-dependent current activation at an internal pH of 5.5 reveals a slowly activating current component in the absence of extracellular Cl^-. (*A*) Control currents in the presence of pipette and bath solutions identical to those in Fig. 1*A*, except for the pH of the internal solution, which was adjusted to 5.5 with HCl. (*B*) Current activation was induced in the presence of 5 μM A23187. (*C*) Replacement of the external Cl^- with glutamate revealed an underlying current with slowly activation kinetics similar to that observed in a population of cells in the presence of extracellular Cl^- (Fig. 1*D–F*). (*D*) Instantaneous current *I-V* relationship obtained from measurements of peak tail current amplitude (inset) following a test depolarization to +100 mV for 100 msec. The current reversal potential of −38.3 mV corresponds to that predicted for a H^+-selective current. *I-V* data taken at time indicated by arrow.

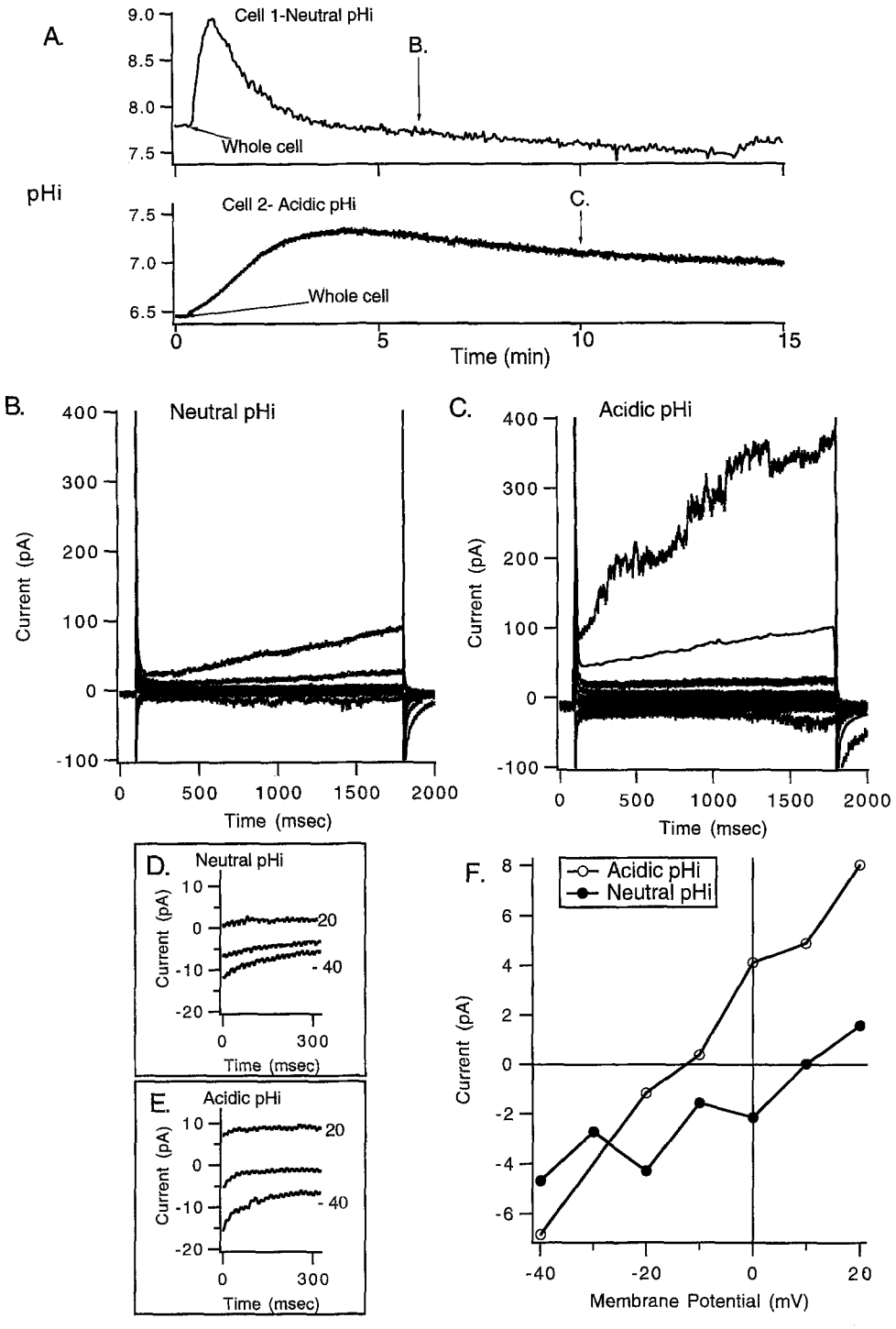

Fig. 4. Simultaneous recording of intracellular pH as monitored by the pH-sensitive dye BCECF and membrane current. (*A*) Time-dependent changes in intracellular pH in two cells following the establishment of the whole-cell recording configuration. In the upper trace labeled *Cell 1*, recordings were made with a pipette solution at neutral pH (pH = 7.2). In the lower trace labeled *Cell 2*, the recording was made in the presence of an acidic pipette solution (pH = 6). The ionic composition of the bath and pipette solutions was identical to that described in Fig. 1*D–F*. (*B*) Whole-cell currents from Cell 1 in the upper trace taken at the time indicated by the arrow. (*C*) Whole-cell currents from Cell 2 in the lower trace taken at the time indicated by the arrow. (*D*) Tail currents for the whole-cell currents depicted in *B* following a depolarizing pulse + 100 mV. (*E*) Tail currents for the whole-cell currents depicted in *C* following a depolarizing pulse + 100 mV. (*F*) Instantaneous current voltage relationships for the tail currents depicted in *D* and *E*. The reversal potential for the currents recorded in Cell 1 at a neutral intracellular pH was 10.0 mV (predicted $E_H = -5.0$) and the reversal potential of the currents recorded in Cell 2 at acidic pH was −12.5 (predicted $E_H = -35.4$).

Time Course and Ca^{2+} Dependence of Current Activation

Current activation following an increase in Ca_i was slow for both Ca^{2+}-dependent conductances and reached maximal levels over a period of approximately 10–20 min (Fig. 5). The delayed time course of activation suggested that a Ca^{2+} regulatory protein could be involved in the process.

The Ca^{2+} dependence of current activation was examined in experiments in which the internal pipette solution was sequentially exchanged in a single cell with solutions buffered to free Ca^{2+} concentrations between 40 and 2,000 nM. Currents obtained in the presence of internal solutions of increasing Ca^{2+} concentrations are illustrated in Fig. 6 for two representative cells. Once maximal current activation had been achieved for either current type in a single cell, further elevation in Ca_i was not associated with either a change in current kinetics nor a large increment in current amplitude suggesting that the conductances were not additive.

Inhibition

Since many anion conductances are inhibited by disulfonic stilbene derivatives, we investigated the effects of the irreversible stilbene DIDS (100 μM). Significant current inhibition in the presence of DIDS was obtained for both current types. Figure 7 illustrates the results of two inhibition experiments carried out on both conductances. DIDS produced a 50.7 ± 7.9% (n = 4) reduction in peak current amplitude at 100 mV for the rapidly activating current and a 75.1 ± 6.0% (n = 5) decrease in peak current amplitude for the slowly activating current.

Ca^{2+}-dependent Chloride Conductance is Phosphorylation Dependent

The lag in current activation for both conductances following an increase in Ca_i (Fig. 5) suggested that channel opening might be occurring through an indirect, phosphorylation-dependent mechanism. To test this hypothesis, we induced current activation in the presence of the nonspecific kinase inhibitor H-7. Inhibition experiments were only carried out on cultures in which Ca^{2+}-dependent current activation was observed in greater than 80% of the cells in the absence of inhibitor.

When the broad spectrum kinase inhibitor H-7 (75 μM) was included in the pipette solution, we were unable to observe current activation for either current type (n = 6) either in the presence of A23187 or in the presence of elevated pipette Ca^{2+} (345 nM). No diminution in current amplitude was observed if H-7 was added to the bathing solution following current activation (n = 2, *data not shown*) indicating that the H-7 effect was not due to a direct channel block. Data obtained in the phosphorylation studies are summarized in Fig. 8.

Multifunctional Ca^{2+}/Calmodulin-dependent Protein Kinase Selectivity Activates the Rapidly Activating Cl^- Conductance

To determine whether the activation of either the Ca^{2+}-dependent Cl^- or H^+ current in the HMDM was mediated via CaMKII, we carried out Ca^{2+}-activation experiments in the presence of the purified kinase and ATP. To avoid the complicating effects of Ca^{2+}, the cell was dialyzed with the kinase which had been autophosphorylated, making its activity independent of Ca^{2+} and calmodulin. Introduction of the autonomous, exogenous kinase to the cell gave rise to current activation over a period of 15–20 min (Fig. 9). Only the rapidly activating Cl^- current was observed following dialysis of the cell with the autophosphorylated kinase. The mean CaMKII-induced current increase at 100 mV, 15 min following whole-cell formation was 1,469 ± 899 pA (n = 4), compared to a mean decrease in current for matched controls over the same time period in the absence of exogenous enzyme of −82 ± 37 pA (n = 4). The zero-current potentials for enzyme-induced currents and control baseline currents were −20.1 ± 8.4 (n = 4) and −12 ± 5.2 mV (n = 4), respectively. The hyperpolarized reversal potential of the CaMKII-induced current indicates that the current was primarily selective for Cl^-.

Discussion

This report is the first to demonstrate Ca^{2+}-dependent activation of both a Cl^-- and a H^+-selective current in macrophages. The Ca^{2+}-dependent Cl^- current showed rapid activation kinetics with an I-V relationship exhibiting some outward rectification in asymmetrical solutions. The H^+-selective current showed delayed activation kinetics upon maintained depolarization with a highly outwardly rectified I-V relationship. The threshold for H^+ current activation shifted with changes in E_H, reminiscent of the shift in activation threshold with E_K observed for inwardly rectifying K^+ channels (Hagiwara & Yoshii, 1979). The H^+-selective current bears similarity in its selectivity and kinetic fingerprint to the zinc-sensitive current with delayed activation kinetics (I_D) described in our previous studies (Nelson et al., 1990).

Both Cl^- and H^+ currents were sensitive to the disulfonic acid stilbene DIDS. It is interesting to note that DIDS acts as an inhibitor of neuronal intracellular pH regulation, retarding the rate of recovery from neu-

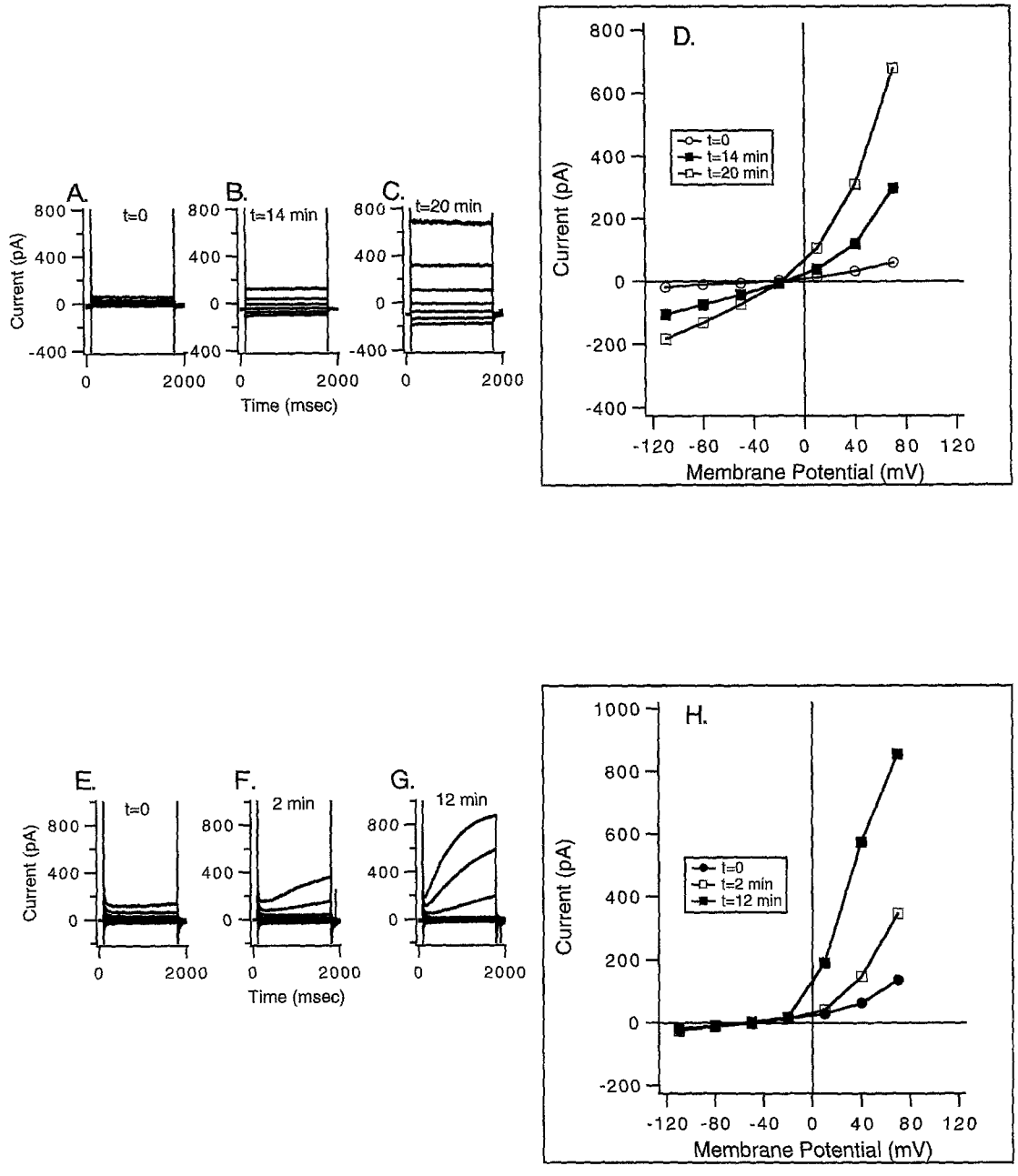

Fig. 5. Delay in maximal conductance activation for both Ca^{2+}-dependent conductances in the presence of an elevated Ca_i. (*A*) Current recording with a pipette solution buffered to a free Ca^{2+} concentration of 100 nM, immediately following the formation of the whole-cell configuration. (*B*) Current activation at 14 min following whole-cell formation. (*C*) Current recording at 20 min, when current activation was maximal. (*D*) *I-V* relationship for the currents in *A* through *C;* control currents prior to activation (open circles), currents 14 min following whole-cell formation (filled squares), and currents at 20 min (open squares) after a stable level of current activation had been maintained. (*E*) Current recording from a second cell in the presence of an internal pipette solution buffered to 100 nM free Ca^{2+}. (*F*) Current activation 2 min later. (*G*) Current activation at 12 min. (*H*) Peak *I-V* relationship for the currents in *E* through *G;* filled circles correspond to control currents prior to activation, open squares correspond to currents activated at 2 min, and filled squares correspond to maximum current activation at 12 min.

rotransmitter-induced acidification in hippocampal cells (Hartley & Dubinsky, 1993). A portion of the inhibitory effect of DIDS on rebound alkalinization in neurons might be due to the block of a similar H^+-selective current.

Ca^{2+}-dependent H^+ current activation appeared to be dependent upon the Ca^{2+}-buffering capacity of the pipette solution, with current activation more frequently observed in solutions containing a relatively low concentration of Ca^{2+} buffer. It is conceivable that in

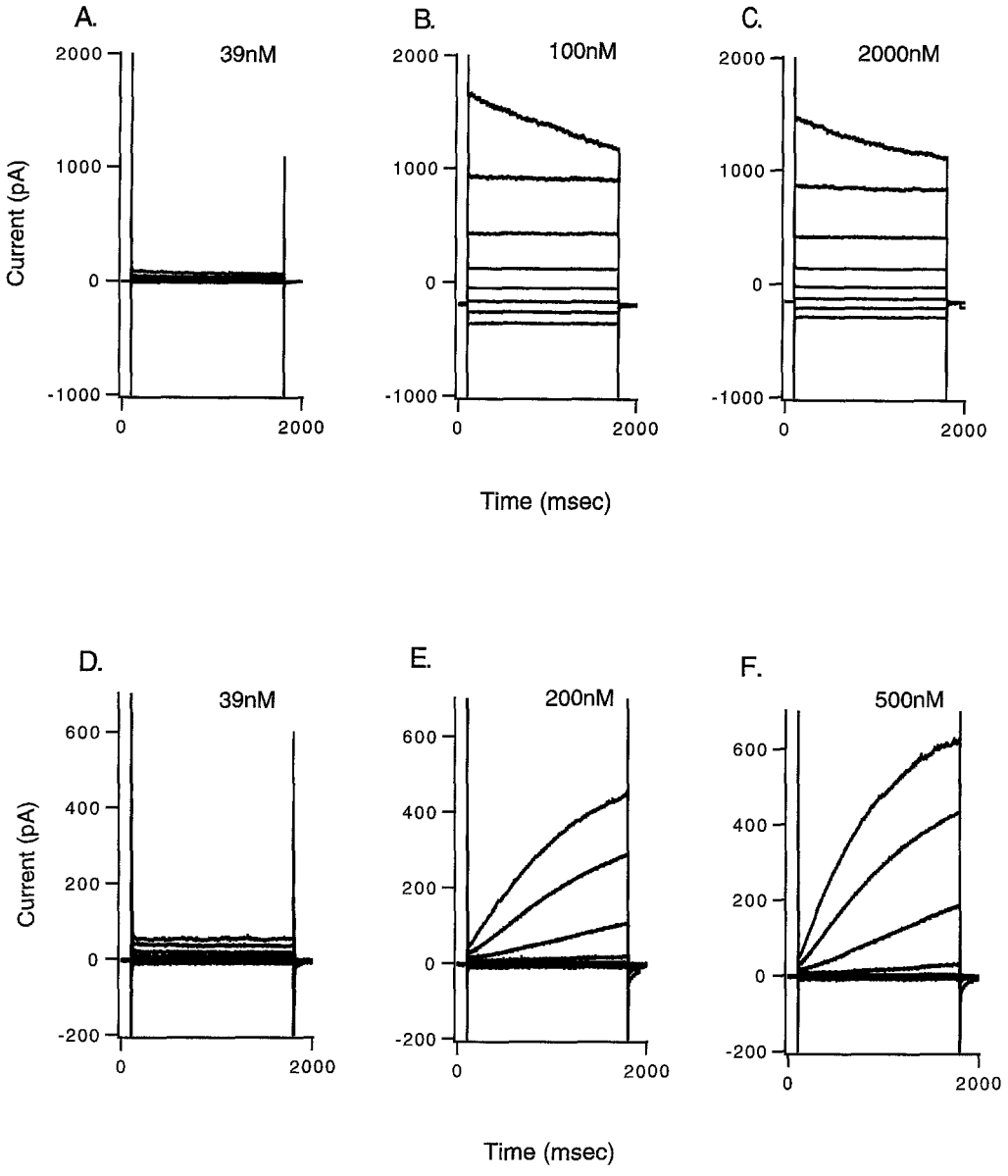

Fig. 6. Further elevation of Ca_i following maximal current activation is not associated with a change in current kinetics for either Ca^{2+}-dependent conductance. (*A–C*) A cell perfused internally with solutions ranging in free Ca^{2+} concentration from 39 to 2,000 nM. (*A*) Current recording in the presence of an intracellular pipette solution buffered to a free Ca^{2+} concentration of 39 nM. (*B*) The pipette solution was exchanged for one buffered to a free Ca^{2+} concentration of 100 nM. (*C*) Current following exchange of the pipette solution for one buffered to a free Ca^{2+} concentration of 2,000 nM. (*D–F*) Current recording from a different cell using a series of intracellular pipette solutions buffered to free Ca^{2+} concentrations of from 39 to 500 nM. (*D*) Current in the presence of 39 nM intracellular Ca^{2+}. (*E*) Current following exchange of the pipette solution for one buffered to a free Ca^{2+} concentration of 200 nM. (*F*) Exchanging the pipette solution for one buffered to a free Ca^{2+} concentration of 500 nM was associated with an increase in peak current magnitude without a change in current kinetics.

cells dialyzed with low intracellular EGTA concentrations, pH_i buffering is reduced in the presence of a large increase in Ca_i. An increase in intracellular proton concentration would produce a hyperpolarizing shift in both E_H as well as the apparent threshold for current activation. A direct correlation between increases in Ca_i and changes in pH_i has been observed in neurons where intracellular iontophoresis of Ca^{2+} leads to cytosolic acidification (Meech & Thomas, 1977, 1980). Based on the studies of Meech and Thomas (1977, 1980), the decrease in pH_i in neurons during trains of action potentials has been attributed to depolarization-induced Ca^{2+} influx. The increase in Ca_i during periods of prolonged excitation is postulated to displace H^+ from intracellu-

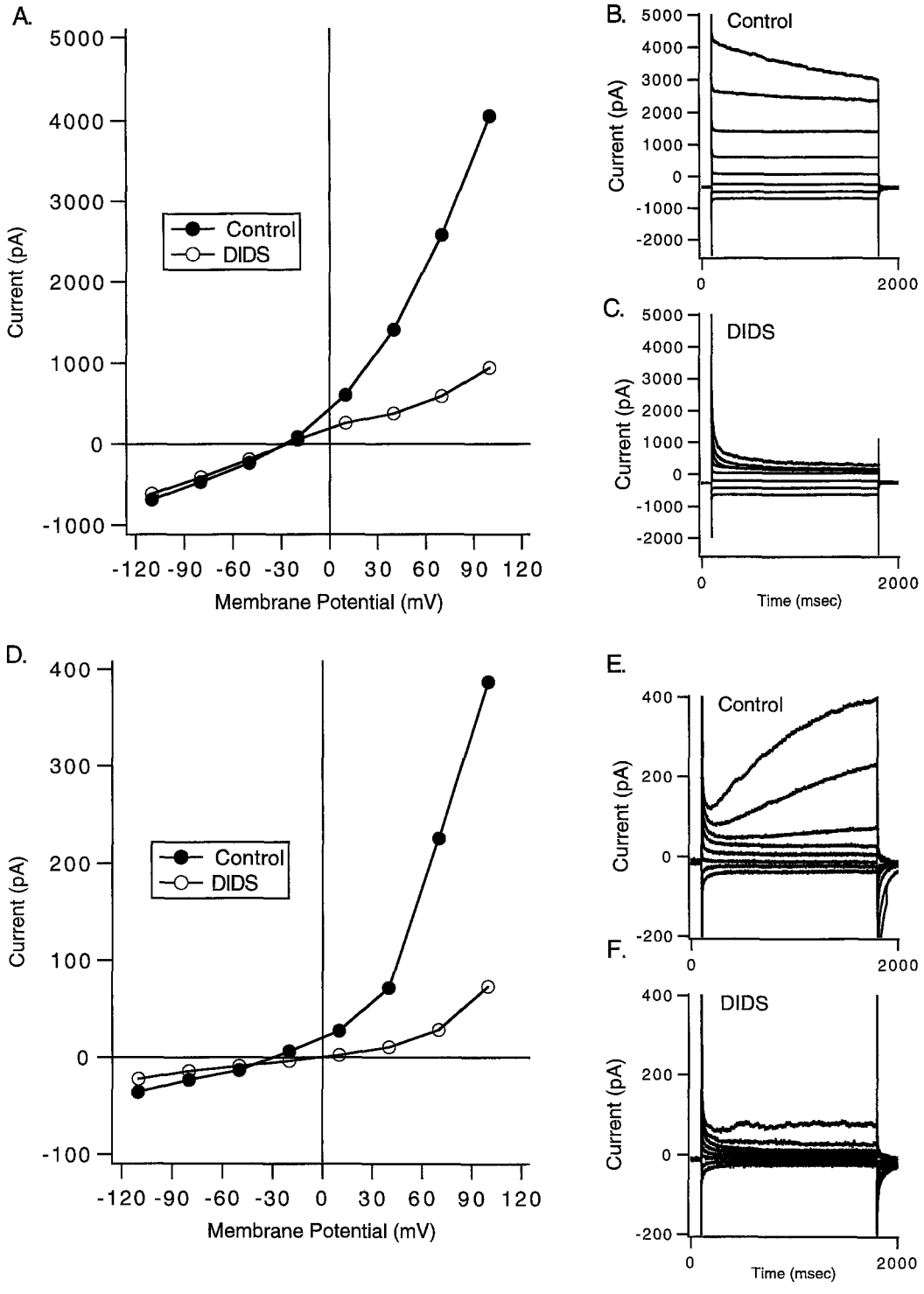

Fig. 7. Inhibition of both Ca^{2+}-dependent currents by the Cl^- channel blocker DIDS (100 μM). (*A–C*) Chloride currents evoked in the presence of an intracellular solution containing 1.0 mM EGTA and 0.2 mM Ca^{2+} (free Ca^{2+} calculated to be 43 nM) (*A*) Peak *I-V* relationship for currents following activation in the presence of elevated Ca_i (filled circles) and for currents in the presence of DIDS (open circles). (*B*) Corresponding whole-cell Cl^- current recorded activated following exposure of the cell to 5 μM A23187. (*C*) Currents following exchange of the bath solution for one containing DIDS (100 μM) which produced significant outward current inhibition. The zero current potential was −28.4 mV for the fully activated current and −26.8 mV in the presence of DIDS. (*D–F*) H^+ currents evoked in the presence of a pipette solution containing 0.45 mM EGTA and 0.3 mM Ca^{2+}. (*D*) Peak *I-V* relationship for currents following activation in the presence of elevated Ca_i (filled circles) and for currents in the presence of DIDS (open circles). (*E*) H^+ current activated in the presence of an intracellular solution containing 345 nM free Ca^{2+}, pH_i = 7.2. (*F*) H^+ currents following exchange of the bath solution for one containing 100 μM DIDS. The zero current potential was −29 mV for the fully activated current and 0 mV in the presence of DIDS.

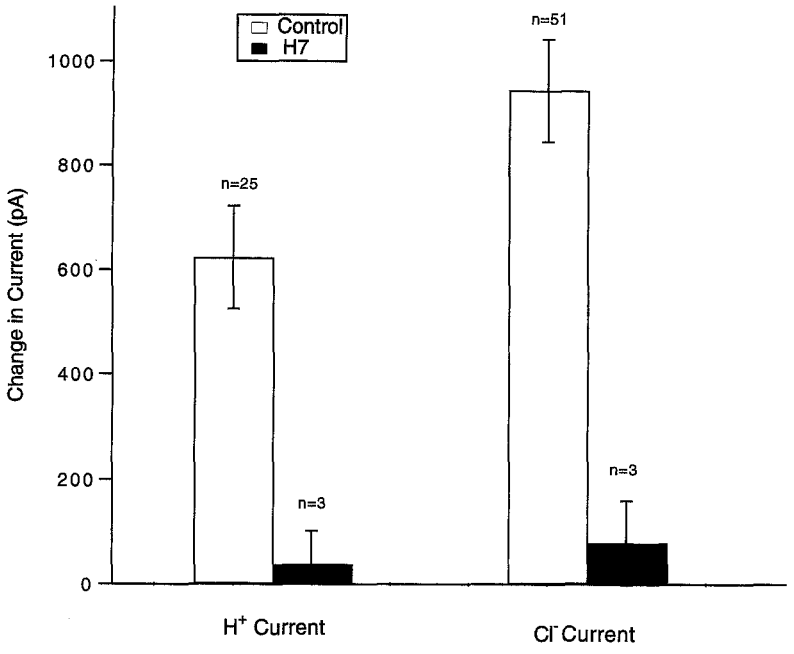

Fig. 8. Effect of H-7 on the activation of both Ca^{2+}-dependent currents. Each bar represents mean current ± SEM recorded at +100 mV. Basal currents prior to maximal Ca^{2+}-dependent current activation were subtracted. Control data represent the mean peak current amplitude for each current type in the absence of inhibitor (open bar). Mean current amplitude for each type of Ca-dependent current is shown following A23187-induced current activation in the presence of intracellular H-7 (filled bars).

lar binding sites as well as enhance Ca^{2+}/H^+ exchange across intracellular Ca^{2+} storage organelles, including mitochondria, thereby bringing about cellular acidification (Thomas, 1989).

Cl^- Channel Phosphorylation as a Mediator of Activation

Our results demonstrate that the Ca^{2+}-dependent activation of both Cl^- and proton conductances is not due to Ca^{2+} binding directly to the channels involved but rather is mediated by a secondary Ca^{2+}-dependent effector molecule. Current activation, regardless of channel type, reached a maximum over a period of minutes, consistent with an enzyme-mediated event rather than direct channel activation. Broad spectrum protein kinase inhibition in the presence of H-7 demonstrates that Ca^{2+}-dependent current activation is phosphorylation dependent. H-7 itself did not alter the current magnitude following activation, demonstrating that these Ca^{2+}-dependent channels are not directly inhibited by the kinase inhibitor. High concentrations (300 μM) of the kinase inhibitor H-7 have been shown to produce voltage-dependent open-channel block of *N*-methyl-D-aspartate receptor channels in cultured hippocampal neurons and muscle nicotinic acetylcholine receptors expressed in *Xenopus* oocytes (Amador & Dani, 1991; Reuhl et al., 1992).

Although activation of both Ca^{2+}-dependent currents was dependent upon phosphorylation, only the Cl^- current was observed in the presence of exogenous, autophosphorylated CaMKII. The H^+ current appears to be regulated by a second unidentified kinase. Multifunctional Ca^{2+}/calmodulin-dependent protein kinase (CaMKII) has been shown to mediate the Ca^{2+}-dependent activation of Cl^- channels in a number of cell types including secretory epithelial cells (Wagner et al., 1991; Worrell & Frizzell, 1991; Chan, Goldstein & Nelson, 1992) and lymphocytes (Nishimoto et al., 1991). Dialysis of HMDMs with isolated CaMKII that had been previously autophosphorylated, thus rendering its activity independent of Ca^{2+} and calmodulin, led to the activation of Cl^--selective currents similar to those elicited via increases in Ca_i. We were unable to identify the kinase involved in the activation of the proton currents in this study. In contrast to our data, the activation of H^+ currents in a number of cells in which they have been characterized, e.g., neurons (Byerly et al., 1984), oocytes (Barish & Baud, 1984), alveolar cells (DeCoursey, 1991), and neutrophils (DeCoursey & Cherny, 1993), does not appear to be either Ca^{2+} or phosphorylation dependent. However, phorbol esters activate electrogenic H^+ efflux in neutrophils (Henderson, Chappell & Jones 1987, 1988; Nanda & Grinstein, 1991; Kapus, Szazi & Ligeti, 1992) suggesting a protein kinase C dependent phosphorylation step in the activation process. The apparent dependence of proton conductance activation on Ca^{2+} and phosphorylation, as demonstrated in our studies, may be indirect and involve Ca^{2+}-dependent activation of NADPH oxidase and/or a number of H^+ transporters involved in the generation of intracellular protons during the respiratory burst in activated macrophages.

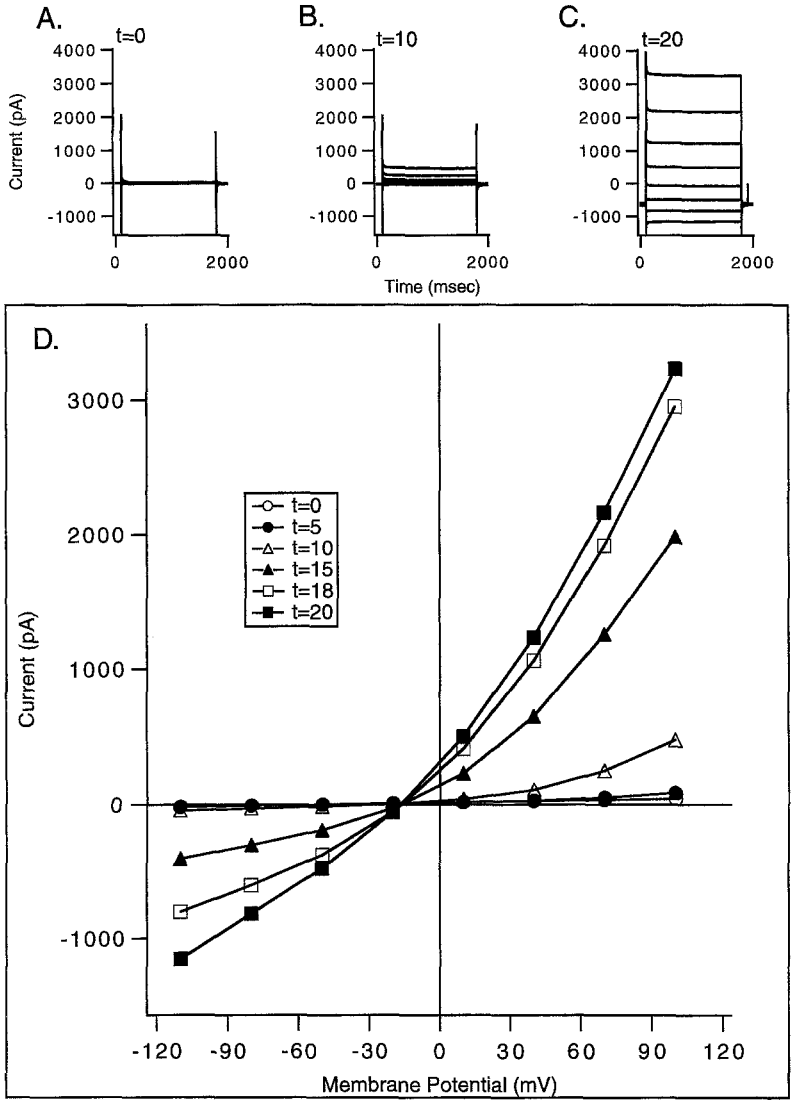

Fig. 9. Cl^- current activation in the presence of autonomous, exogenous CaMKII. Experiments were carried out in standard 140 mM NMDG-Cl bath solutions. The composition of the final pipette buffer solution was: 40 mM NMDG-Cl, 100 NMDG-glutamate, 1 mM Mg-ATP, 2 mM $MgCl_2$, 1 EGTA, 0.2 $CaCl_2$, 10 HEPES and approximately 20 μg/ml CamKII, 60 μM calmodulin, 6 mM PIPES, and 50 μM ATP-γ-S. (*A–C*) Current activation over time after whole-cell formation. (*D*) *I-V* relationship of peak current activated by CaMKII over a 20 min time period.

Ca^{2+}-dependent Channels in Cells of the Immune System

Ca^{2+}-activated K^+ channels have been described in macrophages (Gallin, 1984, 1989; Randriamampita & Trautmann, 1987; Gallin & McKinney, 1988; Nelson et al., 1990) and lymphocytes (Mahaut-Smith & Mason, 1991; Grissmer, Lewis & Cahalan, 1992). Activation of Ca^{2+}-activated K^+ channels in mitogen-stimulated T lymphocytes may maintain a negative membrane potential and thereby be the driving force that regulates Ca^{2+} influx through mitogen-stimulated Ca^{2+} influx pathway(s).

Ca^{2+}-activated Cl^- channels have been characterized in neutrophils (Krause & Welsh, 1990; Schumann, Gardner & Raffin, 1993), T lymphocytes (Nishimoto et al., 1991), and platelets (Mahaut-Smith, 1990). In their analysis of the conductive properties of the plasma membrane of neutrophil granulocytes, Krause and Welsh (1990) postulated that activation of this conductance could contribute to the depolarization observed in neutrophils in response to the Ca^{2+}-mobilizing agonist FMLP, and further, that the depolarization response could serve as an inhibitory signal limiting degranulation and oxygen radical release during activation. Ca^{2+}-dependent Cl^- currents in neutrophils activated in the presence of 1 μM ionomycin and 0.2 mM cytoplasmic EGTA in the studies of Krause and Welsh (1990) did not exhibit time-dependent kinetics over depolarizations of 500 msec and displayed an outwardly rectifying *I-V* relationship. Krause and Welsh did not investigate whether Ca^{2+}-dependent g_{Cl} activation in the neutrophil was direct or indirect via a cytoplasmic kinase.

Recently, Cl^- channels have been identified as a possible link in the signal transduction pathway coupling cytokine binding to neutrophil membranes and the subsequent induction of activation (Schumann et al., 1993). Schumann and colleagues (1993) demonstrated that increases in Ca_i induced by the binding of tumor necrosis factor to neutrophil membranes activated a Ca^{2+}-dependent Cl^- current and that the multifunctional Ca^{2+}-calmodulin dependent kinase (CaMKII) played a role in current activation.

CaMKII has also been shown to mediate the activation of Cl^- channels in Jurkat T lymphocytes (Nishimoto et al., 1991). Treatment of Jurkat T lymphocytes with 100 nM A23187 in the presence of extracellular Ca^{2+} and with pipette solutions containing 0.5 mM EGTA evoked slowly activating outward current with an outwardly rectified *I-V* relationship. In agreement with our experiments, Nishimoto and coworkers observed perceptible current activation approximately one minute following exposure of cells to the Ca^{2+} ionophore, which reached a maximum around 10 min later. Ca^{2+} ionophore-activated current in the lymphocyte was reduced by 66% in the presence of cytoplasmic CaMKII inhibitory peptide.

Cl^- Channels and Their Relationship to Cellular Activation

Cl^- channels are involved in a number of functions in cells in the immune system, including regulation of cell volume, secretion, and cell-mediated cytotoxicity. Gray and Russell (1986) were the first to observe that cytolytic function in murine T lymphocytes was inhibited by isosmotic replacement of extracellular Cl^- with several membrane-impermeant Cl^- substitutes. The loss of cytolytic function in the absence of extracellular Cl^- was attributed to alterations in membrane potential leading to diminished function. It has been proposed that the depolarization observed in neutrophils in response to the chemotactic peptide FMLP, which when bound to surface receptors induces Ca^{2+} mobilization, is due to the activation of a Ca^{2+}-dependent g_{Cl} (Krause & Welsh, 1990).

A Ca^{2+} influx that is triggered during cellular swelling has been observed in a number of cell types (Wong & Chase, 1986; McCarty & O'Neil, 1991*a,b;* Montrose-Rafizadeh & Guggino, 1991) and may occur in macrophages. It has been proposed that the initial swelling causes an influx of Ca^{2+} through mechanosensitive channels, thereby activating neighboring Ca^{2+}-dependent channels, e.g., K^+ and Cl^-, to produce an increase in ion efflux which drives the loss of cell water (Christensen, 1987).

Stimulation of mast cells by externally applied agonists has been shown to activate a slowly developing Cl^- current which is indirectly activated by Ca_i and cAMP (Matthews, Neher & Penner, 1989). This conductance appears to be the largest in the stimulated mast cell and as such is responsible for setting a negative resting potential following stimulation. Matthews and colleagues (1989) have proposed that the Cl^- conductance provides an enhanced driving force for the entry of Ca^{2+} following agonist stimulation, thereby dramatically enhancing the rate of mast cell secretion.

H^+ Ion Currents in Cells in the Immune System

The regulation and functional properties of proton conductances observed in a variety of cell types have been recently reviewed by Lukacs and colleagues (1993). They observe that this pathway may be particularly important in the regulation of pH_i in phagocytes. H^+ currents similar to those we describe in the HMDM have been characterized in the human neutrophil (DeCoursey & Cherny, 1993). The respiratory burst which plays an important role in macrophage microbicidal and tumoricidal activity is accompanied by a burst of intracellular H^+ production that can lead to a drop in pH_i of up to 5 units in fully activated neutrophils within minutes of activation (Nanda & Grinstein, 1991). A pH-regulatory mechanism, therefore, is essential in phagocytic cells. The H^+ conductance, which we observed in the HMDM is activated upon decreases in pH_i, would allow for the effective translocation of protons in the face of rapid cytosolic acidification.

In summary, stimulus-induced Ca_i transients in macrophages appear to activate, in addition to previously described K^+ currents, a Cl^--selective current and a H^+-selective current which differ in their voltage dependence and kinetic properties. While the activation of both currents is Ca^{2+} and phosphorylation dependent, the cytoplasmic enzymes involved in the activation pathways are divergent. Activation of both currents would contribute to ion homeostasis and regulate pH_i as intracellular acid is generated during respiratory burst.

The authors wish to thank Dr. H. Schulman for providing us with the purified CaMKII and Jennifer Foss for technical assistance. This work was supported by National Institutes of Health RO1 GM36823.

References

Amador, M., Dani, J. 1991. Protein kinase inhibitor, H-7, directly affects NMDA receptor channels. *Neurosci. Lett.* **124:**251–255

Barish, M.E., Baud, C. 1984. A voltage-gated hydrogen ion current in the oocyte membrane of the axolotl, *Ambystoma. J. Physiol.* **352:**243–263

Byerly, L., Meech, R., Moody, W. 1984. Rapidly activating hydro-

gen ion currents in perfused neurons of the snail, *Lymnaea stagnalis. J. Physiol.* **351:**199–216

Byerly, L., Suen, Y. 1989. Characterization of protein currents in neurons of the snail, *Lymnaea stagnalis. J Physiol.* **413:**75–89

Chan, H.-C., Goldstein, J., Nelson, D.J. 1992. Alternate pathways for chloride conductance activation in normal and cystic fibrosis airway epithelial cells. *Am. J. Physiol.* **262:**C1273–C1283

Christensen, O. 1987. Mediation of cell volume regulation by Ca^{2+} influx through stretch-activated channels. *Nature* **330:**66–68

Conrad, G.W., Rink, T.J. 1986. Platelet activating factor raises intracellular calcium ion concentration in macrophages. *J. Cell Biol.* **103:**439–450

Decoursey, T.E. 1991. Hydrogen ion currents in rat alveolar epithelial cells. *Biophys. J.* **60:**1243–1253

Decoursey, T.E., Cherny, V. 1993. Potential, pH, and arachidonate gate hydrogen ion currents in human neutrophils. *Biophys. J.* **65:**1590–1598

Fabiato, A., Fabiato, F. 1979. Calculator programs for computing the composition of the solutions containing multiple metals and ligands used for experiments in skinned muscle cells. *J. Physiol. (Paris)* **79:**463–505

Gallin, E.K. 1984. Calcium- and voltage-activated potassium channels in human macrophages. *Biophys. J.* **46:**821–825

Gallin, E.K. 1989. Evidence for a Ca-activated inwardly rectifying K channel in human macrophages. *Am. J. Physiol.* **257:**C77–C85

Gallin, E.K., McKinney, L.C. 1988. Patch-clamp studies in human macrophages: Single channel and whole-cell characterization of two K^+ conductances. *J. Membrane Biol.* **103:**55–66

Gray, L.S., Russell, J.H. 1986. Cytolytic T lymphocyte effector function requires plasma membrane chloride flux. *J. Immunol.* **136:** 3032–3037.

Grissmer, S., Lewis, R.S., Cahalan, M.D. 1992. Ca^{2+}-activated K^+ channels in human leukemic T cells. *J. Gen. Physiol.* **99:**63–84

Hagiwara, S., Yoshii, M. 1979. Effects of internal potassium and sodium on the anomalous rectification of the starfish egg as examined by internal perfusion. *J. Physiol.* **292:**251–265

Hamill, O.P., Marty, A., Neher, E., Sakmann, B., Sigworth, F.J. 1981. Improved patch-clamp techniques for high resolution current recording from cells and cell-free membrane patches. *Pfluegers Arch.* **391:**85–100

Hara, N., Ichinose, M., Sawada, M., Moeno, T. 1991. The activation of Ca^{2+}-dependent K^+ conductance by adrenaline in mouse peritoneal macrophages. *Pfluegers Arch.* **419:**371–379

Hartley, Z., Dubinsky, J.M. 1993. Changes in intracellular pH associated with glutamate excitotoxicity. *J. Neurosci.* **13:**4690–4699

Henderson, L.M., Chappell, J.B., Jones, O.T.G. 1987. The superoxide-generating NADPH oxidase of human neutrophils is electrogenic and associated with an H^+ channel. *Biochem. J.* **246:**325–329

Henderson, L.M., Chappell, J.B., Jones, O.T.G. 1988. Internal pH changes associated with the activity of NADPH oxidase of human neutrophils: further evidence for the presence of an H^+ conducting channel. *Biochem. J.* **251:**563–567

Jaconi, M.E.E., Lew, D.P., Carpentier, J.-L., Magnusson, K.E., Sjögren, M., Stendahl, O. 1990. Cytosolic free calcium elevation mediates the phagosome-lysosome fusion during phagocytosis in human neutrophils. *J. Cell Biol.* **110:**1555–1564

Kapus, A., Szazi, K., Ligeti, E. 1992. Phorbol 12-myristate 13-acetate activates an electrogenic H^+-conducting pathway in the membrane of neutrophils. *Biochem. J.* **281:**697–701

Katnik, C., Nelson, D.J. 1993. Platelet activating factor-induced increase in cytosolic calcium and transmembrane current in human macrophages. *J. Membrane Biol.* **134:**213–224

Kolb, H.-A., Ubl, J. 1987. Activation of anion channels by zymosan particles in membranes of peritoneal macrophages. *Biochim. Biophys. Acta* **899:**239–246

Krause, K.H., Welsh, M.J. 1990. Voltage-dependent and Ca^{2+}-activated ion channels in human neutrophils. *J. Clin. Invest.* **85:**491–498

Kruskal, B.A., Maxfield, F.R. 1987. Cytosolic free calcium increases before and oscillates during frustrated phagocytosis in macrophages. *J. Cell Biol.* **105:**2685–2693

Lew, D.P., Andersson, T., Hed, J., Di Virgilio, F., Pozzan, T., Stendahl, O. 1985. Ca_i-dependent and Ca^{2+}-independent phagocytosis in human neutrophils. *Nature* **315:**509–512

Lipton, S.A., 1986. Antibody activates cationic channels via second messenger Ca^{2+}. *Biochim. Biophys. Acta* **856:**59–67

Lukacs, G.L., Kapus, A., Nanda, A., Romanek, R., Grinstein, S. 1993. Proton conductance of the plasma membrane: properties, regulation, and functional role. *Am. J. Physiol.* **265:**C3–C14

Mahaut-Smith, M.P. 1990. Chloride channels in human platelets: evidence for activation by internal calcium. *J. Membrane Biol.* **118:** 69–75

Mahaut-Smith, M.P., Mason M.J. 1991. Single channel recordings of Ca^{2+}-activated K^+ channels in rat thymic lymphocytes: activation by concanavalin A. *J. Physiol.* **439:**513–528

Matthews, G., Neher, E., Penner, R. 1989. Chloride conductance activated by external agonists and internal messengers in rat peritoneal mast cells. *J. Physiol.* **418:**131–144

McCarty, N.A., O'Neil, R.G. 1991*a*. Calcium-dependent control of volume regulation in renal proximal tubule cells: I. Swelling-activated Ca^{2+} entry and release. *J. Membrane Biol.* **123:**149–160

McCarty, N.A., O'Neil, R.G. 1991*b*. Calcium-dependent control of volume regulation in renal proximal tubule cells: II. Roles of dihydropyridine-sensitive and -insensitive Ca^{2+} entry pathways. *J. Membrane Biol.* **123:**161–170

Meech, R.W., Thomas, R.C. 1977. The effect of calcium injection on the intracellular sodium and pH of snail neurons. *J. Physiol.* **265:** 867–879

Meech, R.W., Thomas, R.C. 1980. Effect of measured calcium chloride injections on the membrane potential and pH of snail neurons. *J. Physiol.* **298:**111–129

Montrose-Rafizadeh, C., Guggino, W. B. 1991. Role of intracellular calcium in volume regulation by rabbit medullary thick ascending limb cells. *Am. J. Physiol.* **260:**F402–F409

Nanda, A., Grinstein, S. 1991. Protein kinase C activates on H^+ (equivalent) conductance in the plasma membrane of human neutrophils. *Proc. Natl. Acad. Sci. USA* **88:**10816–10820

Neher, E. 1988. The influence of intracellular calcium concentration on degranulation of dialysed mast cells from rat peritoneum. *J. Physiol.* **395:**193–214

Nelson, D.J., Jow, B., Jow, F. 1990. Whole-cell currents in macrophages: I. Human monocyte-derived macrophages. *J. Membrane Biol.* **117:**29–44

Nishimoto, I., Wagner, J.A., Schulman, H., Gardner, P. 1991. Regulation of Cl^- channels by multifunctional CaM kinase. *Neuron* **6:** 547–555

Randriamampita, C., Bismuth, G., Trautmann, A. 1991. Ca^{2+}-induced Ca^{2+} release amplifies the Ca^{2+} response elicited by inositol trisphosphate in macrophages. *Cell. Regul.* **2:**513–522

Randriamampita, C., Trautmann, A. 1987. Ionic channels in murine macrophages. *J. Cell Biol.* **105:**761–769

Reuhl, T.O.K., Amador, A., Moorman, J.R., Pinkham, J., Dani, J.A. 1992. Nicotinic acetylcholine receptors are directly affected by agents used to study protein phosphorylation. *J. Neurophysiol.* **68:** 407–416

Schumann, M.A., Gardner, P., Raffin, R.A. 1993. Recombinant human tumor necrosis factor α induces calcium oscillation and cal-

cium-activated chloride current in human neutrophils. *J. Biol. Chem.* **268:**2134–2140

Soejima, M., Noma, A. 1984. Mode of regulation of the ACh-sensitive K-channel by the muscarinic receptor in rabbit atrial cells. *Pfluegers Arch.* **400:**424–431

Thomas, R.C. 1989. Proton channels in snail neurons. Does calcium entry mimic the effects of proton influx? *Ann. NY Acad. Sci.* **574:** 287–293

Wagner, J.A., Cozens, A.L., Schulman, H., Gruenert, D.C., Stryer, L., Gardner, P. 1991. Activation of chloride channels in normal and cystic fibrosis airway epithelial cells by multifunctional calcium/calmodulin-dependent protein kinase. *Nature* **349:**793–796

Wong, S.M.E., Chase, H.S., Jr. 1986. Role of intracellular calcium in cellular volume regulation. *Am. J. Physiol.* **250:**C841–C852

Worrell, R.T., Frizzell, R.A. 1991. CaMKII mediates stimulation of chloride conductance by calcium in T84 cells. *Am. J. Physiol.* **260:** C877–C882